Articles

Induced Peptide Conformations in Different Antibody Complexes: Molecular Modeling of the Three-Dimensional Structure of Peptide–Antibody Complexes Using NMR-Derived Distance Restraints†

Tali Scherf, Reuben Hiller,‡ Fred Naider,§ Michael Levitt, and Jacob Anglister*

Department of Structural Biology, The Weizmann Institute of Science, Rehovot 76100, Israel

Received December 28, 1991; Revised Manuscript Received May 1, 1992

ABSTRACT: Intramolecular interactions in bound cholera toxin peptide (CTP3) in three antibody complexes were studied by two-dimensional transferred NOE spectroscopy. These measurements together with previously recorded spectra that show intermolecular interactions in these complexes were used to obtain restraints on interproton distances in two of these complexes (TE32 and TE33). The NMR-derived distance restraints were used to dock the peptide into calculated models for the three-dimensional structure of the antibody combining site. It was found that TE32 and TE33 recognize a loop comprising the sequence VPGSQHID and a β-turn formed by the sequence VPGS. The third antibody, TE34, recognizes a different epitope within the same peptide and a β-turn formed by the sequence IDSQ. Neither of these two turns was observed in the free peptide. The formation of a β-turn in the bound peptide gives a compact conformation that maximizes the contact with the antibody and that has greater conformational freedom than α-helix or β-sheet secondary structure. A total of 15 antibody residues are involved in peptide contacts in the TE33 complex, and 73% of the contact area in the antibody combining site consists of the side chains of aromatic amino acids. A comparison of the NMR-derived models for CTP3 interacting with TE32 and TE33 with the previously derived model for TE34 reveals a relationship between amino acid sequence and combining site structure and function. (a) The three aromatic residues that interact with the peptide in TE32 and TE33 complexes, Tyr 32L, Tyr 32H, and Trp 50H, are invariant in all light chains sharing at least 65% identity with TE33 and TE32 and in all heavy chains sharing at least 75% identity with TE33. Although TE34 differs from TE32 and TE33 in its fine specificity, these aromatic residues are conserved in TE34 and interact with its antigen. Therefore, we conclude that the role of these three aromatic residues is to participate in nonspecific hydrophobic interactions with the antigen. (b) Residues 31, 31c, and 31e of CDR1 of the light chain interact with the antigen in all three antibodies that we have studied. The amino acids in these positions in TE34 differ from those in TE32 and TE33, and they are involved in specific polar interactions with the antigen. (c) CDR3 of the heavy chain varies considerably both in length and in sequence between TE34 and the two other anti-CTP3 antibodies. These changes modify the shape of the combining site and the hydrophobic and polar interactions of CDR3 with the peptide antigen.

Interest in the molecular interactions of antibodies with peptide antigens has been greatly stimulated by the potential to use synthetic peptides in the production of vaccines (Arnon, 1986; Steward & Howard, 1987). Immunization of animals with short flexible peptides elicits the production of a spectrum of antibodies differing in their affinities to the peptides and the native proteins from which the peptides were derived. Currently there is only limited structural information about antibody–peptide complexes and the conformations of the bound peptide. The three-dimensional structure of an antibody complex with a peptide of myohemerythrin was solved recently by Stanfield et al. (1990), and NMR[1] spectroscopy was used to derive a model for an antibody complex with a cholera toxin peptide (Zilber et al., 1990).

To increase our understanding of the molecular basis for the cross-reactivity of anti-peptide antibodies with native

† This work was supported by a grant from the U.S.–Israel Binational Science Foundation (88-00450) to J.A. and by a grant from the Minerva Foundation, Munich, Germany, to M.L.

* Correspondence should be addressed to this author. He is the incumbent of the Graham and Rhona Beck Career Development Chair.

‡ Levi Eshcol Postdoctoral Fellow. Present address: Department of Biochemistry and Biophysics, 338 Anatomy Chemistry Building, University of Pennsylvania, Philadelphia, PA 19104-6059.

§ Fulbright Exchange Scholar. Present address: The College of Staten Island, The City University of New York, St. George Campus, 130 Stuyvesant Place, Staten Island, NY 10301.

[1] Abbreviations: CDR, complementarity determining region of the antibody molecule; COSY, 2D *J*-correlated spectroscopy; CTP3, cholera toxin peptide 3; DQF-COSY, double-quantum-filtered COSY; ELISA, enzyme-linked immunosorbent assay; ESR, electron spin resonance; Fab, antibody fragment made of the Fv, the light chain, and the first heavy chain constant regions; Fv, antibody fragment made of the variable regions of the light and heavy chains forming a single-combining site for antigen; HLT, heat-labile toxin; NMR, nuclear magnetic resonance; NOE, nuclear Overhauser effect; NOESY, 2D NOE spectroscopy; rms, root mean square; TFE, trifluoroethanol; TRNOE, transferred NOE; V_H, variable region of the heavy chain; 2D, two dimensional; 2D TRNOE difference spectrum, calculated 2D difference spectrum between the measured NOESY spectrum of the protein saturated with the ligand and that of the protein in the presence of a large excess of ligand. Name convention: (a) specific peptide residue, lower-case letters and the position in the sequence (e.g., gln^7); (b) specific antibody residue, capital and lower-case letters and the position in the sequence (e.g., Tyr 32L); H, heavy chain residues; L, light chain residues. The numbering of antibody residues is according to Chothia and Lesk (1987).

0006-2960/92/0431-6884$03.00/0

proteins, it is necessary to study the conformation of the peptide when it is free in solution, when it is part of the native protein, and when it is bound to different antibodies. Such studies should address the following questions: (1) How does the conformation of the bound peptide compare to its conformation in solution and to that of the corresponding epitope in the native protein? (2) What are the implications of these conformational comparisons on the efficacy of the vaccine and on the mechanism by which anti-peptide antibodies are elicited? (3) What is the size of the antigenic determinant recognized by different antibodies, and what are the interactions between the antibodies and the peptide antigen? (4) How do peptide–antibody interactions compare with protein–antibody interactions? Considerable knowledge on the latter topic has been gained from recent crystallographic studies (Amit et al., 1986; Sheriff et al., 1987; Colman et al., 1987; Padlan et al., 1989).

To address these issues, we are studying the interactions of monoclonal antibodies with the peptide (CTP3) corresponding in sequence to residues 50–64 (VEVPGSQHIDSQKKA) of the B-subunit of cholera toxin and the heat-labile toxin of *Escherichia coli*. In vitro, serum of animals immunized with CTP3 partially neutralizes the biological activity of both the cholera toxin and the heat-labile toxin of *E. coli* (Jacob et al., 1983, 1984). Three anti-CTP3 antibodies, TE32 and TE33 which cross-react with cholera toxin in a solid-phase immunosorbent assay (ELISA) and TE34 which does not bind the toxin at all, were selected for detailed NMR investigation (Anglister et al., 1988).

In our studies we use the Fab fragment of the antibody. This fragment has a molecular weight of 50 000 and is too big for a complete structure determination by NMR. However, a knowledge of the three-dimensional structure of the whole complex may not be necessary to address the above issues concerning antibody–antigen interactions and the conformation of the bound antigen. We previously used two-dimensional TRNOE difference spectroscopy to study the interactions of the three antibodies (TE32, TE33, and TE34) with CTP3 (Anglister et al., 1989; Levy et al., 1989; Anglister & Zilber, 1990). Here we present a TRNOE study of intramolecular interactions in bound CTP3 in the three antibody complexes and a study of the free peptide conformation. NMR data on intermolecular and intrapeptide interactions are translated into NMR restraints on interproton distances which are then used to calculate models for the peptide complexed with TE32 and TE33. As a template for docking the peptide, we use a calculated model for the antibody Fv that relies on the three-dimensional structure of a highly homologous anti-progesterone antibody (Deverson et al., 1987; Stura et al., 1987). The conformation of the bound peptide in TE32 and TE33 complexes is compared to its conformation in three other forms: (a) in complex with the TE34 antibody (Zilber et al., 1990), (b) free in solution, and (c) as a segment of HLT (Sixma et al., 1991). The amino acid sequences of TE32 and TE33 are compared to those of highly homologous antibodies with different specificities. These comparisons provide insight on the molecular basis for antibody specificity.

MATERIALS AND METHODS

Materials. Cholera toxin was purchased from Sigma. The following deuterated amino acids were obtained from MSD isotopes: L-tryptophan-*2,4,5,6,7*-d_5 (96.9% D), L-4-hydroxyphenyl-d_4-alanine-*2,3,3*-d_3 (tyrosine) (96.9% D), L-4-hydroxyphenyl-*2,6*-d_2-alanine-*2*-d_1, and L-phenyl-d_5-alanine-*3,3*-d_2 (98% D). A partially deuterated tryptophan, L-tryptophan-*4,6,7*-d_3 (60% H in positions 2 and 5 and 90% D in positions 4, 6, and 7), was a generous gift from Dr. Mei Whittaker, Stanford University. In all measurements, Fab fragments of the antibodies were used. Antibody labeling, Fab preparation, and peptide synthesis and purification were as previously described (Anglister et al., 1989; Anglister & Zilber, 1990).

Synthesis of a Spin-Labeled Peptide (TEMPO-VEVPG-SQHIDSQ). 1-Oxy-2,2,6,6-tetramethyl-4-isothiocyanatopiperidine (ITC-TEMPO) was prepared according to Gaffney (1976). The peptide VEVPGSQHIDSQ (430 mg) was dissolved in a minimal volume of water (5 mL), and the pH was adjusted to 9.6 by addition of triethylamine (approximately 100 mL). The peptide solution was added slowly to a vigorously stirred solution of ITC-TEMPO (300 mg) in dimethylformamide (2 mL). The pH of the reaction mixture was maintained at 9.6 by the addition of small aliquots of triethylamine. After addition of the peptide, the reaction mixture was stirred at room temperature for 24 h. Excess ITC-TEMPO was precipitated by the addition of 70 mL of water and removed by centrifugation. The supernatant was concentrated by partial evaporation and then loaded on a Sephadex G-15 column equilibrated with ammonium carbonate (10 mM). The peptide was further purified by HPLC using a gradient of 2-propanol in an aqueous solution of 10 mM ammonium carbonate. A purity of at least 98% was obtained. The peptide composition and sequence were verified by amino acid analysis and the NMR spectra of the spin-labeled peptide before and after reduction with sodium dithionite.

Measurements of Binding Constants by Fluorescence Quenching. The binding constant of TE33 for the spin-labeled peptide was measured as previously described by following the quenching of the Fab fluorescence upon peptide binding (Anglister et al., 1988). The Fab fluorescence was measured at room temperature on a Perkin-Elmer MPF-44E fluorescence spectrophotometer. The excitation wavelength was 283 nm with a slit bandwidth of 2 nm, and the emission was measured at 363 nm with a slit bandwidth of 15 nm. Fab concentration was 10^{-6} M. The Fab fluorescence was measured as a function of the added concentration of the spin-labeled peptide. The required correction for the nonspecific absorption of the spin-labeled peptide at the absorption and emission wavelengths of Fab fluorescence was found by measuring the decrease in the fluorescence of the tryptophan solution caused by the addition of the spin-labeled peptide.

Measurement of TE33 Binding to Cholera Toxin by ESR. ESR spectra were measured on a Varian E-12 spectrometer. A calibration curve for the peak height versus the concentration of spin-labeled peptide was obtained. Spectra of 25 μM spin-labeled peptide in the presence of 25 μM TE33 Fab without and with 143 μM cholera toxin were measured (Figure 1, spectra A and B, respectively). Due to a much shorter correction time the free peptide has a sharp resonance separated from the broad signal of the bound peptide. The concentration of the free peptide was deduced from the peak height of its signal marked as free in spectrum A (Figure 1).

Sample Preparation for NMR Measurements. NOESY spectra of TE33 Fab in D_2O were measured at 42 °C and pH 7.15. Fab concentration was originally 2.8 mM and was reduced to 2.2 mM after the addition of a 4-fold CTP3 excess. In 90% H_2O/10% D_2O (v/v) solution, TE33 Fab concentration was 3.0 mM after addition of a 7-fold peptide excess, and the pH was 5.5. Measurements in 90% H_2O/10% D_2O were carried out at 15 °C. TE34 Fab (1.7 mM) in 90% H_2O/10% D_2O solution containing 300 mM NaCl was measured at 39

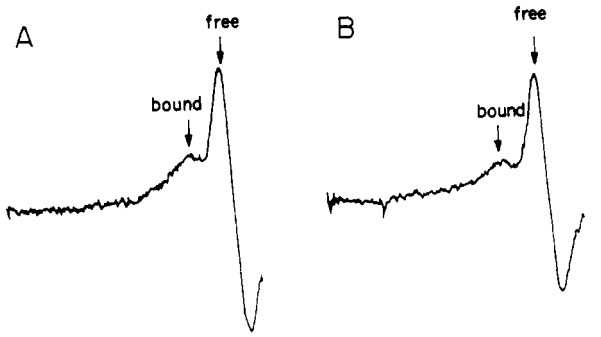

FIGURE 1: (A) ESR spectrum of 25 μM TEMPO-VEVPGSQHIDSQ in the presence of an equimolar concentration of TE33 Fab in phosphate-buffered saline at room temperature and pH 7. The signals of the free and bound spin-labeled peptide are indicated in the figure. (B) The same spectrum after the addition of 143 μM cholera toxin.

°C and pH 4.15, and a 3-fold peptide excess was used. Spectra of 15 mM free CTP3 in 90% H_2O/10% D_2O (v/v) solution were measured at pH 3.95 and 4 °C. All solutions were buffered with 10 mM sodium phosphate.

NMR Measurements. All spectra were measured on a Bruker AM500 spectrometer using the phase-sensitive mode. The procedure for difference spectra calculations as well as for NOESY measurements in D_2O solutions was described previously (Anglister et al., 1989; Anglister & Zilber, 1990). In the DQF-COSY (Piantini et al., 1982) measurements of the Fab in the presence of peptide excess, the H_2O line was presaturated by selective irradiation during the preparation period before the 90° excitation pulse was applied. For each of 400 increments of t_1 we collected 16 scans with 8K data points in the t_2 domain. In NOESY measurements of H_2O solutions of the Fab–peptide complexes, the carrier frequency was set on the H_2O line and the 1–1 jump–return pulse sequence was used for selective excitation (Plateau & Gueron, 1982). The NOESY spectra (Macura & Ernst, 1980) of the Fab in the presence of peptide excess were recorded at a mixing time of 100 ms for the TE33 Fab–peptide complex and at 100 and 200 ms for the TE34 Fab–peptide complex. Typically, 64 or 80 scans of 2K data points were collected for 400–440 t_1 increments. For the NOESY and the DQF-COSY measurements of the CTP3 peptide, 600 t_1 values were recorded with 8K data points along t_2; 32 scans were collected for each t_1 value. The mixing time used in the NOESY measurement of the peptide was 400 ms. In the measurements of the peptide spectra, the H_2O line was supressed by presaturation.

RESULTS

TE33 Binding to Cholera Toxin. TE33 binding to cholera toxin was determined by using ESR spectroscopy to follow the competition between cholera toxin and the spin-labeled version of CTP3 (TEMPO-VEVPGSQHIDSQ). In these measurements, the resonance of the free peptide appears as a narrow signal while that of bound peptide is broadened due to the slower rotational correlation time of the complex (see Figure 1). The binding constant of TE33 Fab for the spin-labeled peptide was calculated from measurements of the free peptide concentration as a function of the total concentration of the spin-labeled peptide added to 25 μM TE33 Fab, giving a value of 0.9×10^6 M^{-1}. The ESR measurements were used also to calibrate the peak height of the bound peptide signal versus its concentration. As an alternative and to confirm the ESR measurements, the binding constant of TE33 Fab for the spin-labeled peptide was also determined by a fluorescence quenching procedure (see Materials and Methods) and was found to be 1.2×10^6 M^{-1}. This value is identical to that for

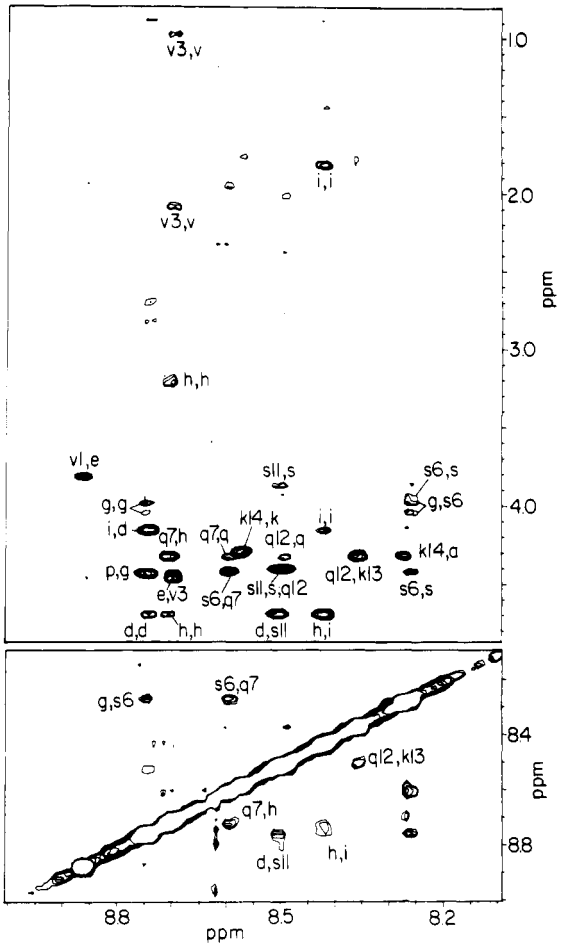

FIGURE 2: A section of the NOESY spectrum of free CTP3 (VEVPGSQHIDSQKKA) in H_2O showing interactions of amide protons with other protons in the peptide. The spectrum was measured at 4 °C and pH 3.95.

CTP3 (VEVPGSQHIDSQKKA) (Anglister et al., 1988) and is in good agreement with the ESR measurements. Very high concentrations of the toxin were necessary to obtain measurable changes in the ratio between the concentrations of the bound and free spin-labeled peptide. Addition of 0.143 mM cholera toxin (each molecule contains five B-subunits) resulted in a 20% increase in the ratio between the free and the bound peptide (Figure 1B). The measurements were repeated five times, and the average calculated binding constant of the toxin was found to be $(1 \pm 0.5) \times 10^3$ M^{-1}, which is 3 orders of magnitude weaker than TE33 binding for the spin-labeled peptide.

Intramolecular Interactions in Free CTP3. As shown in Figure 2, the NOESY spectrum of CTP3 reveals several intraresidue interactions, all of the strong sequential [$(\alpha(i)$–$N(i+1))$] interactions, and several very weak interactions between the amide protons of adjacent residues [$N(i)$–$N(i+1)$]. The multiple amide–amide interactions are confined to the sequence between gly^5 and lys^{13} of CTP3 and are too weak to reflect any significant population of a helical conformation or the presence of reverse turns. The peptide resonances were assigned on the basis of the DQF-COSY and the NOESY spectra.

Intrapeptide Interactions in the Complexes of TE33 and TE32 with CTP3. Figure 3A presents a section of the 2D TRNOE difference spectrum showing TRNOE cross-peaks due to intramolecular interactions between nonaromatic protons of CTP3 bound to TE33. Tryptophan and phenylalanine residues of the antibody were perdeuterated, and ty-

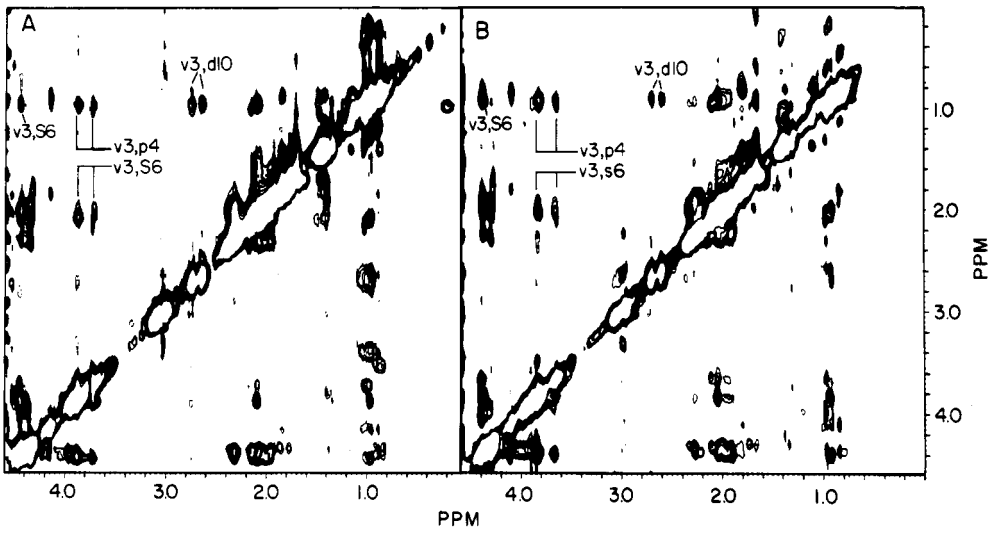

FIGURE 3: (A) Difference between the NOESY spectrum of TE33 Fab with a 4-fold excess of CTP3 and that of the TE33 Fab saturated with CTP3 showing intramolecular interactions of aliphatic protons in the bound peptide. Spectra were measured in phosphate-buffered D_2O at 42 °C and pH 7.15 with 100-ms mixing time. Antibody tyrosine C_δ protons were deuterated, and tryptophan and phenylalanine residues were perdeuterated. (B) The corresponding difference spectrum obtained for TE32 under conditions identical to those in (A).

rosine C_δ protons were deuterated to minimize spin diffusion. The two strong cross-peaks at 0.96, 3.72 and 0.96, 3.87 ppm are assigned to interactions of val[3] methyl protons with the δ protons of pro[4]. The first of these peaks overlaps a weaker cross-peak due to intraresidue interaction in val[1], and the second of these peaks overlaps an even weaker cross-peak due to interaction between ser[6] $C_\beta H$ and val[3] CH_3. The cross-peaks at 3.84, 2.08 and 3.88, 2.08 ppm are due to interaction of ser[6] β protons with val[3] $C_\beta H$. These two cross-peaks overlap a stronger cross-peak due to intraresidue interaction in pro[4]. These assignments are based on (a) the COSY spectrum of free CTP3 and of a truncated version of CTP3 comprising residues 1–10, (b) disappearance of cross-peaks upon deuteration of val[3], (c) considerable decrease in intensity on pro[4] deuteration, and (d) the fact that all these cross-peaks are not affected by deuteration of glu[2] and gln[7]. The two cross-peaks at 0.96, 2.64 and 0.96, 2.74 ppm are assigned to interactions between val[3] CH_3 and asp[10] C_β protons. This assignment is based on (a) chemical shifts identical to those of the corresponding free peptide resonances, (b) their multiplicity, and (c) disappearance on deuteration of val[3]. Although distant in sequence, the val[3] and asp[10] protons are adjacent in the bound peptide, indicating loop formation. Previous observation of an antibody Trp proton (W) and Tyr C_ϵ protons (Y1) interacting with both val[3] CH_3 and asp[10] β protons provides additional evidence for this loop (Anglister et al., 1989). Similar interactions in the bound peptide were observed for the TE32–CTP3 complex (Figure 3B). Some of the cross-peaks in Figure 3 are not symmetrical due to different resolution in the F_1 and F_2 dimensions, difficulties in correcting the phases of the columns and rows in the difference spectra, interference of t_1 noise, and baseline distortions.

Intramolecular interactions of the amide protons of the peptide bound to TE33 were studied by transferred NOE measurements in 90% H_2O/10% D_2O. In order to observe the amide protons, it is necessary to slow their exchange with the hydrogen atoms of water while maintaining an off-rate sufficient for measurement of TRNOE. At pH 4, which is optimal for slow amide proton exchange, the peptide binding decreased considerably. To observe amide protons at a higher pH (pH = 5.5), we had to lower the temperature to 15 °C to counterbalance the increase in amide proton exchange due to the elevated pH. However, the decrease in the temperature concomitantly decreased the off-rate. Successful NMR measurements at pH 5.5 had to be carried out using a truncated ligand, VEVPGSQHID-amide. In a previous study (Anglister & Zilber, 1990) we found that this truncated peptide, which retains most of the determinant recognized by TE33, has an off-rate which is an order of magnitude faster than that of CTP3. It was found that this truncation of the peptide did not interfere with the interactions of the remaining peptide residues with the antibody (Anglister & Zilber, 1990). The difference between the NOESY spectrum of the Fab in the presence of excess VEVPGSQHID-NH_2 and that of the Fab in the presence of equimolar peptide concentration was calculated and compared to the NOESY spectrum of the Fab in the presence of excess peptide. Due to the broad line width of the protein amide protons and the large excess of the peptide (7-fold), it was not necessary to calculate a difference spectrum to resolve the TRNOE cross-peaks of the peptide amide protons from background cross-peaks contributed by the protein.

Figure 4 presents a section of the NOESY spectrum of TE33 Fab in the presence of excess VEVPGSQHID-NH_2, showing intramolecular interactions of the amide protons of the bound peptide observed via TRNOE. A very strong TRNOE cross-peak due to interaction between the amide protons of gly[5] and ser[6] is observed. This cross-peak indicates a formation of a β-turn by the sequence VPGS. Some of the interactions that have been shown in Figure 3—Ser[6] β protons interacting with a val[3] β proton and methyl protons, a ser[6] α proton interacting with val[3] methyl protons—support a bend formation. A weaker cross-peak between the amide protons of ile[9] and asp[10] indicates that some bend formation may also occur at the C-terminus of the epitope. In Figure 4, a long-range interaction between the amide proton of asp[10] and the methyl protons of val[3], manifested by a cross-peak at 8.56, 0.94 ppm, further confirms the formation of a loop.

Intramolecular Interactions in the Peptide Bound to TE34. The off-rate of CTP3 bound to TE34 was previously found to be too slow to measure TRNOE (Anglister & Zilber, 1990). Therefore, we used two versions of the peptide which had fast enough off-rates: (a) HIDSQKKA-amide, in which seven N-terminal residues were truncated and the C-terminal carboxyl was modified into an amide, and (b) IDSQRKA, in which eight N-terminal residues were truncated and lys[13] was replaced by arg to avoid degeneracy in chemical shifts. In the latter probe his[8], which is in the determinant recognized by

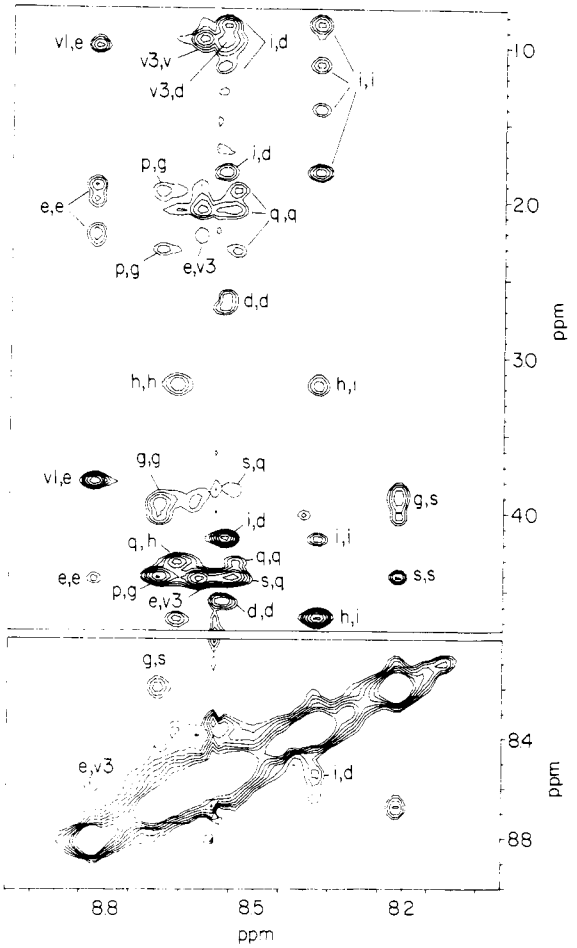

FIGURE 4: NOESY spectrum of TE33 Fab with a 7-fold excess of a truncated version of the CTP3 peptide (VEVPGSQHID-amide) showing intramolecular interactions of the amide protons in the bound peptide. The measurement was done in phosphate-buffered 90% H_2O/10% D_2O at pH 5.5 and 15 °C with 100-ms mixing time. Antibody tyrosine C_δ protons were deuterated, and tryptophan and phenylalanine residues were perdeuterated.

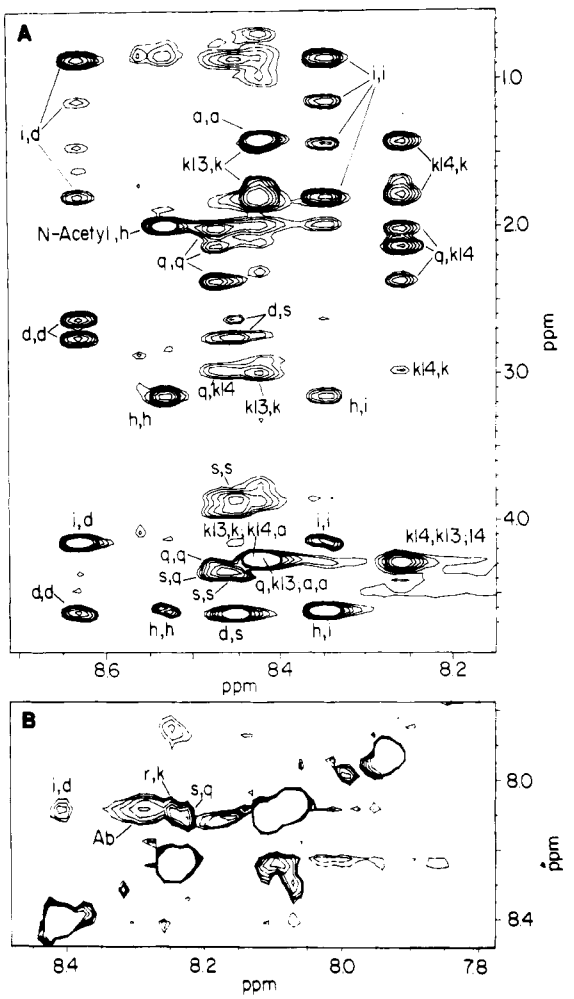

FIGURE 5: (A) NOESY spectrum of TE34 Fab with a 7-fold excess of a truncated version of CTP3 (HIDSQKKA-amide) showing intramolecular interactions of the amide protons of the bound peptide with its other protons. The spectrum was measured in phosphate-buffered 90% H_2O/10% D_2O at 15 °C and pH 5.5 with a mixing time of 100 ms. Tryptophan, phenylalanine, and tyrosine residues of the antibody were perdeuterated. (B) Section of the 2D TRNOE difference spectrum of TE34 using a 3-fold excess of IDSQRKA showing interactions between amide protons of the bound peptide. The spectra were measured in phosphate-buffered 90% H_2O/10% D_2O at 39 °C and pH 4.2 with 200-ms mixing time. TE34 was deuterated as in (A).

TE34 (Anglister & Zilber, 1990), was eliminated, but the C-terminal carboxyl was not modified. We have previously found that these modifications did not interfere significantly either with the interactions of the unmodified part of the peptide with the antibody or with intramolecular interactions occurring in the epitope recognized by the antibody (Anglister & Zilber, 1990). The binding constant of TE34 for its peptide antigen did not decrease even when the pH was lowered to 4.2. To enhance the off-rate of IDSQRKA, measurements with this peptide were carried out at 39 °C. Under these conditions the amide exchange was still slow enough. According to the previously obtained NMR-derived model for the TE34 complex with CTP3, residues IDSQ form a β-turn (Zilber et al., 1990). Such a turn should manifest a strong TRNOE cross-peak between the amide protons of ser^{11} and gln^{12}. However, the 0.05 ppm chemical shift difference between these two resonances in the spectrum of HIDSQKKA-amide prevents the observation of a cross-peak sufficiently well resolved from the diagonal. In IDSQRKA, the chemical shift difference between these two resonances is 0.13 ppm, and cross-peaks should be observed. A section of the two-dimensional TRNOE difference spectrum obtained for TE34 Fab in 90% H_2O/10% D_2O containing a 3-fold excess of IDSQRKA and using 200 ms mixing time is shown in Figure 5B. Tryptophan, phenylalanine, and tyrosine residues of TE34 were perdeuterated to minimize spin diffusion. We observed strong interactions between the amide protons of ser^{11} and gln^{12} and of arg^{13} and lys^{14} and a much weaker interaction between the amide protons of ile^9 and asp^{10}. While the first two interactions are strong in a spectrum measured with 100-ms mixing time, the interaction between ile^9 and asp^{10} is considerably weaker. In the previously derived model for TE34 (Zilber et al., 1990) the protons in these three pairs are separated by distances shorter than 3.1 Å. Figure 5A shows a section of the NOESY spectrum of TE34 in the presence of a 7-fold excess of HIDSQKKA-amide. As the off-rate of this peptide is much faster than that of IDSQRKA, we observe stronger TRNOE cross-peaks due to intramolecular interactions in the bound peptide. Several short-range interresidue interactions were observed. The amide protons of ile^9, asp^{10}, ser^{11}, gln^{12}, and lys^{14} interact with the side chains of his^8, ile^9, asp^{10}, lys^{14}, and gln^{12}, respectively.

Intra-Fab Interactions in TE33. Information concerning the interresidue interactions of residues in the antibody combining site region provides valuable insights into the structure of the binding domain and helps support the assignment of antibody–peptide interactions to specific antibody residues. To obtain this information, we subtracted the 2D NOE

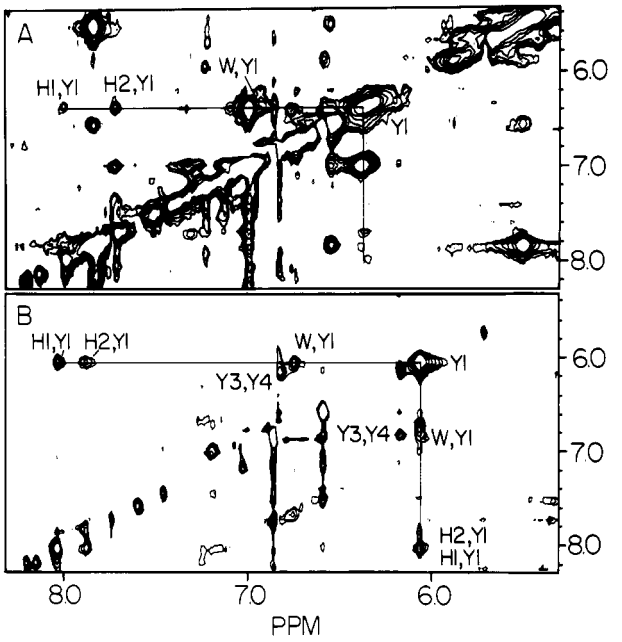

FIGURE 6: Difference between the 2D NOE spectrum of the TE33 Fab with excess CTP3 and that of the uncomplexed Fab showing intramolecular interactions in the antibody as well as intermolecular interactions. Antibody phenylalanine residues are perdeuterated while tyrosine residues are deuterated at the C_δ positions. Tryptophan residues have 40% deuterium at $C_{\zeta 3}$ and $C_{\delta 1}$ and 90% deuterium at the other indole positions. (A) Negative cross-peaks contributed by the TE33–CTP3 complex. (B) Positive cross-peaks contributed by the noncomplexed Fab. Interacting antibody residues are marked by capital letters and arbitrary numbers. Spectra were measured in phosphate-buffered D_2O at 42 °C and pH 7.15 with 100-ms mixing time.

spectrum of the uncomplexed Fab from that of the Fab with excess CTP3 peptide. Cross-peaks in this difference spectrum arise from intramolecular interactions of antibody protons that change chemical shift upon peptide binding, intermolecular interactions between antibody and peptide, and intramolecular interactions in the bound peptide. To obtain a difference spectrum free of the numerous cross-peaks due to intraresidue interactions, tryptophan and tyrosine residues were partially deuterated while phenylalanine residues were completely deuterated. Comparison with a spectrum obtained for TE33 under similar conditions, in which tryptophan and phenylalanine residues were perdeuterated and tyrosine residues deuterated at the $C_{\delta 1}$ and $C_{\delta 2}$ positions, enabled us to assign cross-peaks to their specific amino acid types.

Inspection of both positive and negative cross-peaks allows us to study interactions occurring either in the Fab or in the TE33–CTP3 complex, respectively, (panels B and A of Figure 6). These spectra show strong interaction of Y1 with H1, H2, and W. We previously found that these protons interact with the peptide; Y1 corresponds to Tyr 32L, H1 and H2 to His 31L, and W to $C_{\delta 1}H$ of Trp 100aH (Levy et al., 1989). Additional interactions between the C_ϵ protons of two tyrosine residues (Y3 and Y4) are also observed (Figure 6B). Neither Y3 nor Y4 interacts with CTP3 as judged by a two-dimensional TRNOE difference spectrum showing TE33 tyrosine residue interactions with CTP3 (Anglister et al., 1989). Nevertheless, since their chemical shift changes upon CTP3 binding, they are assumed to be in the combining site region. Specific chain-labeling experiments (Levy et al., 1989) and inspection of the calculated model suggest that Y3 and Y4 are Tyr 100bH and Tyr 49L, respectively. NMR observation of the interactions between combining site residues which are proximal in the model for the antibody Fv provides experimental support for the calculated structure.

Spin Diffusion. In order to rule out the possibility that spin diffusion effects appeared in the 2D TRNOE difference spectra measured with a mixing time of 100 ms, we carried out measurements with different mixing times of 30, 60, and 100 ms. In these measurements we used TE33 Fab in which tryptophan and phenylalanine residues were perdeuterated and tyrosine C_δ protons were deuterated. All cross-peaks due to the interactions of tyrosine C_ϵ and histidine imidazole protons of the antibody were observed at the shorter mixing time, excluding the possibility of spin diffusion. When it was possible to calculate the volume integral accurately, the change in cross-peak intensity as a function of the mixing time ruled out the possibility of a delay in the rise of the NOE cross-peaks. The increase in intensity of two cross-peaks was proportional to the increase in mixing time from 60 to 100 ms. The intensity of all other cross-peaks increased to a considerably lesser extent, and two of them became slightly weaker at the longer mixing time.

NMR Distance Restraints. NMR results from previous studies on intermolecular interactions in the TE32 and TE33 complexes (Anglister et al., 1988, 1989; Levy et al., 1989) together with those presented here were translated into interproton distance restraints using volume integral measurements of the NOESY cross-peaks. The intensity of the strongest cross-peak [designated W-v3 in Anglister et al. (1989) and Levy et al. (1989)] in the difference spectrum between the NOESY spectrum of the Fab in the presence of excess peptide and that of the Fab saturated with the peptide was compared to the intensity of the exchange cross-peak of $C_{\delta 2}H$ of the peptide histidine. Since this cross-peak appears in all TRNOE difference spectra, and as all spectra were measured under the same conditions, at the same mixing time, and with the same molar ratio of peptide–antibody, it can serve as an internal standard for calibrating the intensities of all cross-peaks in all TRNOE difference spectra measured in D_2O solutions. To evaluate the distance between the peptide val^3 methyl protons and the antibody tryptophan proton, we examined the difference spectrum between the NOESY spectrum of Fab with excess peptide and that of the Fab itself measured for TE33 Fab in which tyrosine and phenylalanine were perdeuterated. In addition to the transferred NOE cross-peaks, this difference spectrum contained cross-peaks due to intraresidue interactions of the two tryptophan residues in the combining site since their chemical shifts changed upon peptide binding. From the comparison of the intensity of the W-v3 cross-peak with those of the cross-peaks due to intraresidue interactions between adjacent protons on the tryptophan indole, we concluded that the W-v3 cross-peak corresponds to a distance of about 3 Å. Other cross-peaks were attributed to distances shorter than 3.0, 3.5, 4.0, and 4.5 Å, depending on their relative intensity. In the absence of stereospecific resonance assignments, heavy atoms that are close to the center of the line connecting the two hydrogen atoms were used as pseudoatoms (Wüthrich et al., 1983), and a correction was added to the NOE distance constraint. In a few cases stereospecific assignments were added after preliminary models were calculated using restraints on pseudoatoms. Additional intrapeptide proton–proton distance restraints were obtained from the NOESY spectrum of the TE33 Fab–peptide complex in H_2O (Figure 4). Under the conditions in which this spectrum was measured, we could observe transferred NOE cross-peaks only due to intramolecular interactions in the bound peptide. In the absence of a phenyl group in the peptide, we had to use a cross-peak due to the intra γ-NH_2 protons

of the glutamine residue of the peptide as an internal reference for distance calibration. All the restraints used in our calculations are due to interactions of amide protons (8.2–8.6 ppm) or side-chain protons with chemical shifts between 0.9 and 2.1 ppm. In this range of chemical shift the excitation profile of the 1–1 jump–return pulse reaches its maximum and does not vary to a considerable extent. Therefore, no correction was applied to the measured cross-peak intensity. The lists of the intermolecular distance restraints as well as the intra-bound-peptide distances used in the modeling of the TE33–CTP3 and of the TE32–CTP3 complexes are given in Tables I and II, respectively. All cross-peaks were assigned before calculation of the model for the complex, and the assignments did not require any correction after preliminary calculations. We derived distance restraints for all the assigned cross-peaks, and all of them were used in the calculations.

Calculation of Antibody Models. Models for the antibodies TE32 and TE33 were built as described before with two improvements. (a) The atomic coordinates of the antibody DB3, which is highly homologous to these antibodies (Levy et al., 1989), were used to provide initial coordinates for all the main-chain atoms and the side-chain atoms of homologous residues. (b) A new method was used for the missing side-chain atoms, which are taken from any of the other eight antibody structures that have known X-ray structures in the Brookhaven Protein Data Bank: the six Fab's, KOL (Marquart et al., 1980), NEW (Saul et al., 1978), McPC 603 (Satow et al., 1987), J539 (Suh et al., 1986), HyHel-5 (Sheriff et al., 1987), and HyHel-10 (Padlan et al., 1989), and the two V_L dimers, REI (Epp et al., 1975) and RHE (Furey et al., 1983). Defects in the stereochemistry of these models were eliminated as before by energy minimization using the program ENCAD (Levitt, 1983a). The new models of TE32 and TE33 are better than the models built previously (Levy et al., 1989) using six antibodies known then (KOL, NEW, McPC 603, J539, REI, and RHE) in that they have fewer missing atoms (41 and 47 as opposed to 117 and 126) and lower total energy values after energy refinement (−1717 and −1735 kcal/mol as opposed to −1486 and −1534 kcal/mol). The new structures are very similar to that previously described (Levy et al., 1989) except for the conformation of a segment of CDR2 of the heavy chain starting from Ile 51H. The conformation of Trp 50H, which is shown by NMR to interact with the peptide, is similar in the two models. The possibility that this segment of CDR2 was not modeled correctly in the first models was discussed previously (Zilber et al., 1990). The improvement in the second model arises from using a much more homologous structure of CDR2 in the calculations.

Calculation of the Models of Peptide–Antibody Complexes. The NMR-derived distance restraints and the preliminary models for the antibodies Fv were used to calculate a molecular model for the antigenic determinant VPGSQHID bound to TE32 and TE33. With the powerful molecular graphics program FRODO (Jones, 1978) on an Evans & Sutherland PS390, this sequence was docked into the TE33 combining site by bringing each of its amino acid residues near combining site residues shown by NMR to interact. In all cases reasonable lengths for the peptide bonds were maintained. This initial model of the complex was refined by a combination of restrained energy minimization and molecular dynamics calculations. We used restraints that depend on the fourth power of the difference between NOE and model distance as described before (Zilber et al., 1990).

For macromolecular systems that have many degrees of freedom, minimization with the distance restraints is not generally able to get to the lowest accessible energy minimum. Early studies (Levitt, 1983b) show that running molecular dynamics between energy minimizations is a very effective way to get low energies. The protocol used for annealing dynamics started with minimization consisting of four passes each of 200 steps (here a step is a single evaluation of the energy and its first derivative). This was followed by ten passes each consisting of 10 ps of molecular dynamics (10000 steps each lasting 0.001 ps) at a temperature of 300 K followed

Table I: NMR-Derived Distance Restraints for the TE33 Complex with CTP3

atom i[a]	atom j[a]	distance constraint[b] (Å)	distance in model[c] (Å)	deviation[d] (Å)
val 3 $C_{\gamma 2}$	His 31L $H_{\epsilon 1}$	4.0	4.4	0.4
val 3 H_{α}	His 31L $H_{\epsilon 1}$	3.0	2.8	0.0
val 3 $C_{\gamma 1}$	Tyr 32L $H_{\epsilon 2}$	4.0	4.3	0.3
val 4 $C_{\gamma 1}$	Trp 100aH $H_{\delta 1}$	4.0	4.0	0.0
pro 4 C_{γ}	His 31L $H_{\delta 2}$	4.0	4.7	0.7
pro 4 C_{δ}	His 31L $H_{\delta 2}$	5.0	4.4	0.0
pro 4 C_{δ}	His 31L $H_{\epsilon 1}$	5.0	5.0	0.0
pro 4 $H_{\delta 1}$	Tyr 32L $H_{\epsilon 2}$	4.0	4.4	0.4
pro 4 $H_{\delta 2}$	Tyr 32L $H_{\epsilon 2}$	4.0	4.4	0.4
pro 4 C_{γ}	Tyr 32L $H_{\epsilon 2}$	5.0	5.6	0.6
pro 4 $H_{\beta 2}$	Phe 96L $H_{\epsilon 2}$	3.0	3.7	0.7
pro 4 $H_{\beta 2}$	Phe 96L H_{ζ}	4.0	2.3	0.0
pro 4 $H_{\gamma 1}$	Phe 96L H_{ζ}	4.0	3.9	0.0
pro 4 $H_{\gamma 2}$	Phe 96L $H_{\epsilon 2}$	4.0	4.6	0.6
pro 4 $H_{\gamma 2}$	Phe 96L H_{ζ}	4.0	2.3	0.0
gly 5 C_{α}	Phe 96L $H_{\epsilon 2}$	4.0	4.0	0.0
gly 5 C_{α}	Phe 96L H_{ζ}	4.0	4.0	0.0
gly 5 C_{α}	Trp 50H $H_{\eta 2}$	5.0	3.8	0.0
gln 7 $H_{\gamma 1}$	Trp 50H $H_{\zeta 3}$	3.0	3.6	0.6
gln 7 $H_{\gamma 1}$	Trp 50H $H_{\eta 2}$	3.0	3.0	0.0
gln 7 $H_{\gamma 1}$	Trp 50H $H_{\zeta 2}$	3.0	3.3	0.3
his 8 C_{β}	Tyr 32H $H_{\epsilon 2}$	5.5	6.0	0.5
his 8 $H_{\delta 2}$	Tyr 32H $H_{\epsilon 2}$	4.0	4.3	0.3
his 8 $H_{\epsilon 1}$	Tyr 32H $H_{\epsilon 2}$	4.0	2.7	0.0
his 8 $H_{\epsilon 1}$	Tyr 32H $H_{\delta 2}$	4.0	2.8	0.0
his 8 $H_{\delta 2}$	Trp 100aH $H_{\eta 2}$	3.0	3.1	0.1
his 8 $H_{\delta 2}$	Trp 100aH $H_{\zeta 3}$	3.0	3.4	0.4
his 8 C_{β}	Trp 100aH $H_{\zeta 3}$	6.0	5.5	0.0
his 8 $H_{\delta 2}$	Trp 100aH $H_{\zeta 2}$	3.0	3.5	0.5
his 8 C_{β}	Trp 100aH $H_{\eta 2}$	5.0	4.8	0.0
his 8 C_{β}	Trp 100aH $H_{\zeta 2}$	6.0	3.0	0.0
asp 10 C_{β}	Tyr 32L $H_{\epsilon 2}$	5.5	5.8	0.3
asp 10 C_{β}	Trp 100aH $H_{\delta 1}$	5.5	5.9	0.4
Tyr 32L $H_{\epsilon 2}$	His 31L $H_{\delta 2}$	4.0	3.5	0.0
Tyr 32L $H_{\epsilon 2}$	His 31L $H_{\epsilon 1}$	4.0	4.0	0.0
val 3 $C_{\gamma 1}$	asp 10 $H_{\beta 1}$	4.0	3.0	0.0
val 3 $C_{\gamma 1}$	asp 10 $H_{\beta 2}$	4.0	3.7	0.0
pro 4 $H_{\delta 1}$	val 3 $C_{\gamma 1}$	4.0	3.3	0.0
pro 4 $H_{\delta 2}$	val 3 $C_{\gamma 1}$	4.0	3.7	0.0
gly 5 H	pro 4 $H_{\gamma 2}$	2.5	3.0	0.5
gly 5 H	pro 4 $H_{\beta 2}$	3.0	2.5	0.0
ser 6 C_{β}	val 3 H_{β}	5.0	4.2	0.0
ser 6 H_{α}	val 3 $C_{\gamma 1}$	4.0	4.3	0.3
ser 6 C_{β}	val 3 $C_{\gamma 1}$	6.0	6.1	0.1
ser 6 H	gly 5 H	3.0	2.3	0.0
gln 7 H	val 3 C_{β}	6.0	4.5	0.0
ile 9 $C_{\delta 1}$	asp 10 H	4.0	4.2	0.2
ile 9 $C_{\gamma 1}$	asp 10 H	4.5	4.0	0.0
ile 9 $H_{\gamma 11}$	ile 9 H	3.0	2.5	0.0
ile 9 $H_{\gamma 12}$	ile 9 H	3.0	2.1	0.0
ile 9 H	asp 10 H	3.5	4.3	0.8
asp 10 H	val 3 C_{β}	5.5	5.3	0.0

[a] Peptide residues are written with lower-case letters while antibody residues are written with capital and lower-case letters; H, heavy chain residues; L, light chain residues. [b] The value given reflects the maximum distance from the NOE restraints and additional distance due to the use of pseudoatoms (Wüthrich et al., 1983). [c] The distances in the final model were obtained by energy minimization and molecular dynamics calculations. [d] The deviation is that between the restraint and the actual distance in the model. When the latter is smaller than the restraint, the deviation is set equal to zero.

Table II: NMR-Derived Distance Restraints for the TE32 Complex with CTP3

atom i[a]	atom j[a]	distance constraint[b] (Å)	distance in model[c] (Å)	deviation[d] (Å)
val 3 $C_{\gamma 2}$	His 31L $H_{\epsilon 1}$	4.0	4.6	0.6
val 3 $C_{\gamma 1}$	Tyr 32L $H_{\epsilon 2}$	4.0	4.7	0.7
val 3 $C_{\gamma 1}$	Trp 100aH $H_{\delta 1}$	4.0	3.9	0.0
pro 4 C_{γ}	His 31L $H_{\delta 2}$	4.0	4.1	0.1
pro 4 C_{δ}	His 31L $H_{\delta 2}$	5.5	4.1	0.0
pro 4 C_{δ}	His 31L $H_{\epsilon 1}$	5.5	4.4	0.0
pro 4 $H_{\delta 1}$	Tyr 32L $H_{\epsilon 2}$	4.0	4.6	0.6
pro 4 $H_{\delta 2}$	Tyr 32L $H_{\epsilon 2}$	4.0	4.3	0.3
pro 4 C_{γ}	Tyr 32L $H_{\epsilon 2}$	5.0	5.6	0.6
gly 5 C_{α}	Trp 50H $H_{\eta 2}$	5.5	5.1	0.0
gln 7 C_{γ}	Trp 50H $H_{\eta 2}$	4.0	4.1	0.1
gln 7 C_{γ}	Trp 50H $H_{\zeta 3}$	4.0	4.6	0.6
gln 7 C_{γ}	Trp 50H $H_{\zeta 2}$	4.0	4.3	0.3
his 8 C_{β}	Tyr 32H $H_{\epsilon 2}$	5.5	5.9	0.4
his 8 $H_{\delta 2}$	Tyr 32H $H_{\epsilon 2}$	4.0	3.5	0.0
his 8 $H_{\epsilon 1}$	Tyr 32H $H_{\epsilon 2}$	4.0	3.9	0.0
his 8 $H_{\epsilon 1}$	Tyr 32H $H_{\delta 2}$	4.0	3.4	0.0
his 8 $H_{\delta 2}$	Trp 100aH $H_{\eta 2}$	3.0	3.3	0.3
his 8 $H_{\delta 2}$	Trp 100aH $H_{\zeta 3}$	3.0	3.4	0.4
his 8 C_{β}	Trp 100aH $H_{\zeta 3}$	6.0	5.2	0.0
his 8 C_{β}	Trp 100aH $H_{\eta 2}$	5.0	4.4	0.0
his 8 C_{β}	Trp 100aH $H_{\zeta 2}$	6.0	3.6	0.0
asp 10 C_{β}	Trp 100aH $H_{\delta 1}$	5.5	5.6	0.1
asp 10 C_{β}	Tyr 32L $H_{\epsilon 2}$	5.5	5.8	0.3
Tyr 32L $H_{\epsilon 2}$	His 31L $H_{\delta 2}$	4.0	3.3	0.0
Tyr 32L $H_{\epsilon 2}$	His 31L $H_{\epsilon 1}$	4.0	4.5	0.5
val 3 $C_{\gamma 1}$	asp 10 $H_{\beta 1}$	4.0	3.2	0.0
val 3 $C_{\gamma 1}$	asp 10 $H_{\beta 2}$	4.0	4.4	0.4
pro 4 $H_{\delta 1}$	val 3 $C_{\gamma 1}$	4.0	3.3	0.0
pro 4 $H_{\delta 2}$	val 3 $C_{\gamma 1}$	4.0	3.7	0.0
ser 6 C_{β}	val 3 H_{β}	5.0	4.7	0.0
ser 6 H_{α}	val 3 $C_{\gamma 1}$	4.0	4.5	0.5
ser 6 C_{β}	val 3 $C_{\gamma 1}$	6.0	6.6	0.6

[a] Peptide residues are written with lower-case letters while antibody residues are written with capital and lower-case letters; H, heavy chain residues; L, light chain residues. [b] The value given reflects the maximum distance from the NOE restraints and additional distance due to the use of pseudoatoms (Wüthrich et al., 1983). [c] The distances in the final model were obtained by energy minimization and molecular dynamics calculations. [d] The deviation is that between the restraint and the actual distance in the model. When the latter is smaller than the restraint, the deviation is set equal to zero.

by minimization for 600 steps. Note that the molecular dynamics that followed the energy minimization was continued from the time step immediately preceding the minimization. This gave a single continuous trajectory lasting 100 ps which was sampled by minimization every 10 ps to provide 11 different energy minima. All hydrogen atoms are included in these energy minimization and molecular dynamics calculations using energy parameters given in Levitt (1983a).

Ten models were calculated for the TE33 complex. In these calculations all peptide residues and only a few antibody residues (Phe 96L, Tyr 32H, Arg 95H, Ser 96H, and Trp 100aH) were allowed to move. Tables I and II also give the deviations between the NMR restraints and the distances in the calculated model with the lowest energy. The rms deviation between the 52 NMR restraint distances and the distances in the calculated models for TE33 is 0.32 Å, and the total energy of the restrained interactions is −147.3 kcal/mol. In view of the fact that a model rather than a known crystal structure was used for docking the peptide, the violations of the distance restraints are remarkably low, strongly supporting the high quality of the model and the reliability of the NMR-derived distance restraints. The bound peptide conformation in the ensemble of the calculated models is shown in Figures 7 and 8. The rms deviation between the nine models and the model with the lowest energy is 0.67 Å for the main-chain atoms and 1.0 Å for the side-chain atoms. The averaged rms deviation between the model with the lowest energy and the nine other models for each of the residues of the epitope is given in Figure 9A. The higher dispersion around his[8] is probably a result of the fact that the two antibody residues (Trp 100aH and Tyr 32H) that interact with his[8] were allowed to move. We did not restrain interaction of ile[9] with the antibody, and there are only three restraints on ile[9] interactions with adjacent peptide residues. As a result the conformation of ile[9] is poorly defined. In contrast, the backbone and the side-chain conformation of val[3], pro[4], gln[7], and asp[10] are very well-defined.

Ten models were also calculated in the same way for the TE32 complex, except that residue 96L was not allowed to move (Phe in TE33 is replaced by Leu in TE32). The rms deviation between the 33 NMR restraint distances and the distances in the model with the lowest energy is 0.36 Å, and the total energy of the restrained interactions is −118.6 kcal/mol. Figure 8 shows a comparison between the models for the bound peptide in TE32 and TE33, respectively. Due to a smaller number of distance restraints, the conformational variability in the TE32 complex is considerably greater than that observed in the TE33 complex; however, the peptide assumes very similar conformations in the two antibody complexes. The rms deviation between the nine models and the model with the lowest energy is 1.06 Å for the main-chain atoms and 1.47 Å for the side-chain atoms. The statistics for each of the residues of the epitope is given in Figure 9B.

Description of Structure. Panels A and B of Figure 10 illustrate the models obtained for the CTP3 complexes with TE33 and TE32, respectively. Tables III and IV summarize the contacts in the calculated NMR-derived models between CTP3 and TE33 and TE32, respectively. In the TE33 complex the epitope includes CTP3 residues 3–10 with at least six residues directly interacting with the antibody. The side chains of val[3], pro[4], gly[5], gln[7], and his[8] are buried inside the complex and fill a circular groove around Trp 100aH. The shortest distance between the two ends of the loop formed by the peptide, from the val[3] methyl protons to the asp[10] β protons, is 2.4 Å. The four N-terminal residues of the epitope (VPGS) form a β-turn conformation which is stabilized by a hydrogen bond between the val[3] carbonyl oxygen and the amide proton of ser[6] and a bifurcated hydrogen bond between ser[6] $O_{\gamma}H$ and the val[3] carbonyl. Intramolecular polar interactions are found between the gly[5] NH and the gln[7] $O_{\epsilon 1}$.

Additional intermolecular polar interactions exist between the ser[6] carbonyl oxygen and the Tyr 53H $O_{\zeta}H$, the gln[7] δNH_2 and the guanidinium group of Arg 95H, the gln[7] carbonyl oxygen and the Tyr 53H $O_{\zeta}H$, and the asp[10] O_{δ} and both the Asn 31eL γNH_2 and the His 31L $H_{\delta 1}$ protons. Strong hydrogen bonds are formed between his[8] $N_{\epsilon 2}$ and Ser 96H and between asp[10] $O_{\delta 2}$ and both Tyr 32L $O_{\zeta}H$ and Ser 31cL $O_{\gamma}H$. van der Waals interactions are found between pro[4] $H_{\gamma 1}$ and the Ser 92L carbonyl oxygen and between his[8] $H_{\epsilon 1}$ and the Thr 31H carbonyl oxygen. val[3] has hydrophobic interactions with His 31L, Tyr 32L, and Trp 100aH; pro[4] interacts with His 31L, Tyr 32L, His 93L, Ile 94L, and Phe 96L; gly[5] CH_2 interacts with Ile 94L, Phe 96L, and Trp 50H; gln[7] interacts with Phe 96L, Trp 50H, and Trp 100aH; and the his[8] imidazole is buried in a hydrophobic pocket formed by Tyr 32H and Trp 100aH.

A similar structure obtained for the TE32–CTP3 complex is shown in Figure 10B. The automatic program modeled differently the side chain of Arg 95H in TE32, and as a result the position of the side chain of gln[7] had been changed in the calculated model for the antibody–peptide complex. Ac-

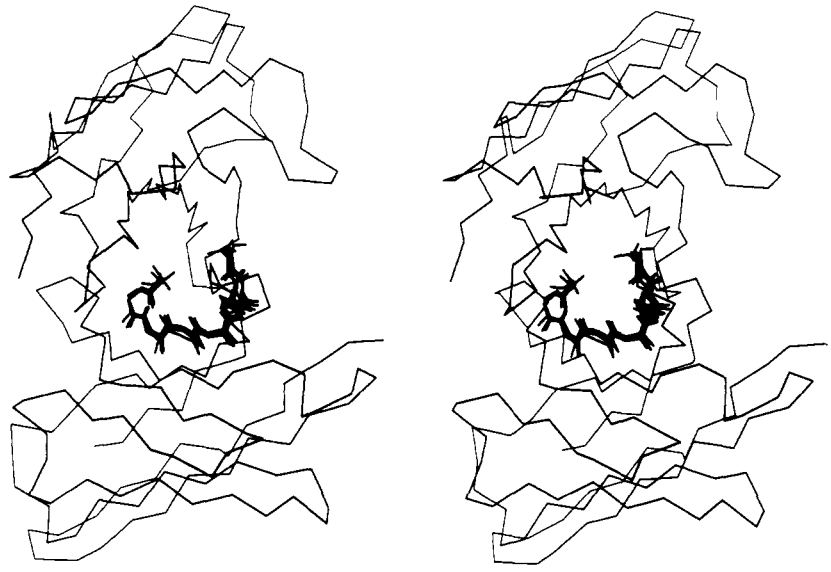

FIGURE 7: Stereoview showing superposition of the five best-fit calculated models for the polypeptide backbone of the segment VPGSQHID bound to TE33.

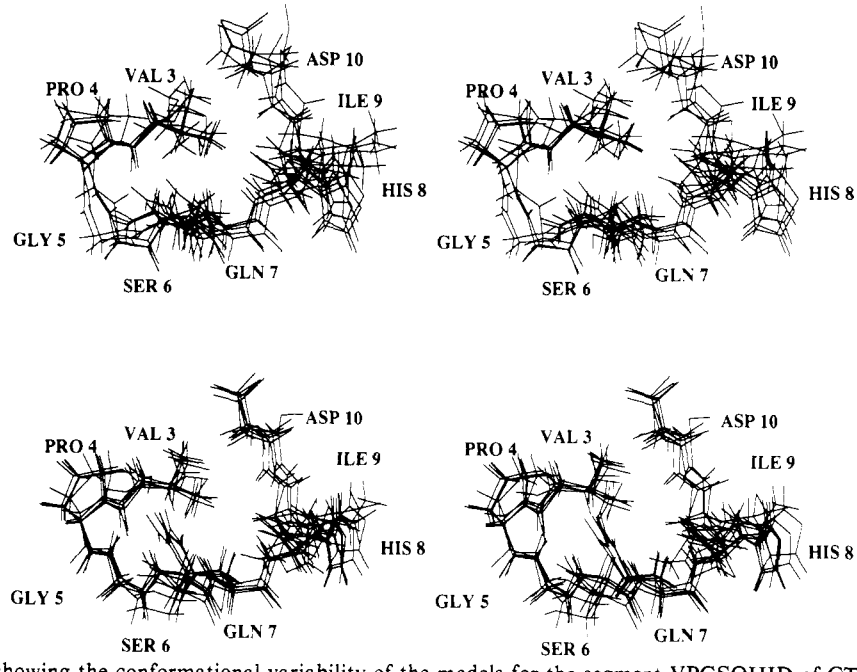

FIGURE 8: Stereoview showing the conformational variability of the models for the segment VPGSQHID of CTP3. The top figure shows the models for the TE32 complex, and the bottom figure shows the models for the TE33 complex. For clarity, only the first six models were drawn.

cordingly, all polar interactions involving the gln[7] side-chain atoms are missing, except for a hydrogen bond between the $O_{\epsilon 1}$ and the gln[7] amide proton (of the polypeptide backbone). A new intrapeptide hydrogen bond is found between the carbonyl oxygen of pro[4] and one of the gln[7] $\delta N H_2$ protons. The β-turn conformation found in the epitope of TE33 is also predicted in TE32 and is stabilized by a hydrogen bond between the NH of ser[6] and the carbonyl oxygen of val[3].

The total contact area between the antibody and the peptide epitope is 406 Å^2 in TE33 and 344 Å^2 in TE32. The total contact area is about half of that observed in antibody–protein complexes (Sheriff et al., 1987; Amit et al., 1986) and is comparable to that previously found for TE34 (Zilber et al., 1990). The side chains of antibody aromatic residues occupy 73% of this contact area. All antibody CDRs except the second CDR of the light chain interact with the peptide. In the peptide bound either to TE32 or to TE33, about half of the contact with the antibody is made by gln[7] and his[8], and most intramolecular contacts are made by val[3]. The peptide conformation is stabilized by folding around val[3], which acts as a hydrophobic core.

The model obtained for CTP3 bound to TE33 when the restraints on the amide proton interactions are not taken into account is very similar to that obtained when all restraints are taken into account and is similar to that obtained for the TE32 complex.

DISCUSSION

The Potential of the TRNOE Technique. This study demonstrates the power of TRNOE measurements to elucidate the conformation of bound ligands and their interactions with large proteins. For proteins exhibiting slow ligand off-rates resulting in weak TRNOE cross-peaks, slight modification or truncation of the ligand can be used to obtain well-resolved 2D TRNOE difference spectra with good signal-to-noise ratios

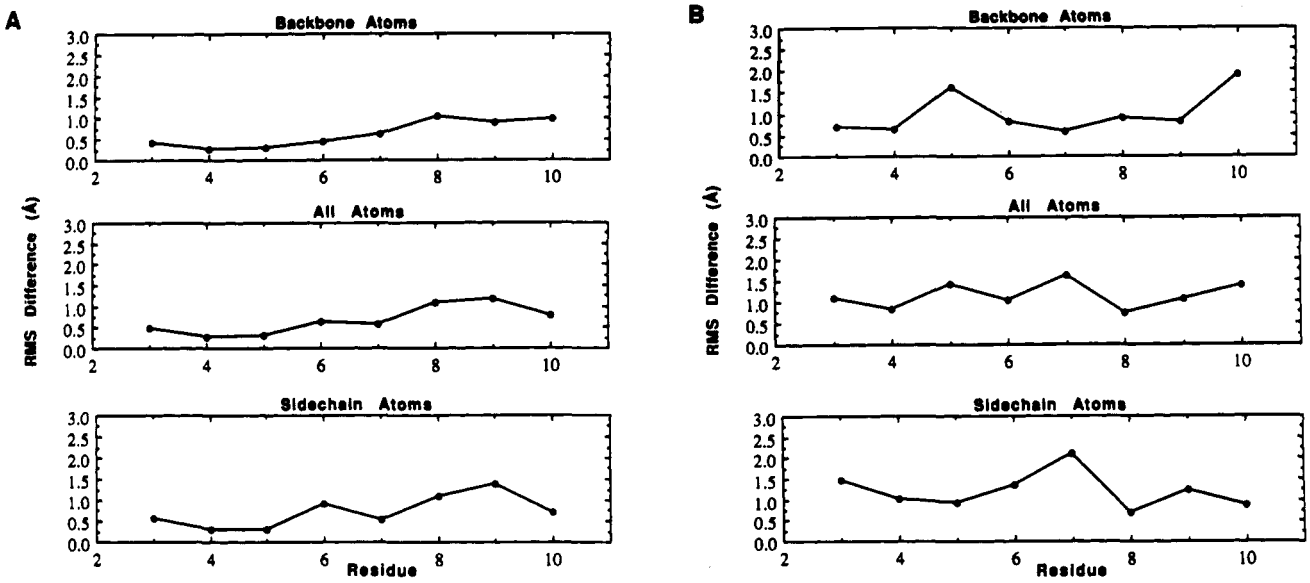

FIGURE 9: Average rms deviation between the model with the lowest energy and the nine other models for backbone atoms, all atoms, and side-chain atoms of the epitope residues. Panels: (A) TE33–CTP3 complex; (B) TE32–CTP3 complex.

(Anglister & Zilber, 1990). Transferred NOE measurements are best applied when the three-dimensional structure of the protein is known, and one is interested in studying the interactions between a protein and its ligand and the bound ligand conformation. However, even in the absence of a solved protein structure, as in our case, a model for the protein can be used successfully.

Modeling of the antibody combining site was found to be very successful in a number of cases in which it could be compared to a solved antibody structure (Chothia et al., 1987, 1989; Padlan et al., 1989). The NMR results are used to verify and refine the initial model for the free protein and to dock the ligand into the combining site as was done in the pioneering work of Dwek and his co-workers (Dwek et al., 1977) and later by McConnell and his co-workers (Anglister et al., 1987; Theriault et al., 1991). In very favorable cases, one can obtain enough NMR restraints on intramolecular distances in the bound ligand to solve its conformation independently of a calculated model (Clore et al., 1986). In our studies we did not resolve a large enough number of intrapeptide NOE distance restraints to permit unequivocal determination of the structure of bound CTP3. Enough data were obtained to qualitatively describe the conformation of bound CTP3 peptide: a loop and a β-turn formed by the sequence VPGS in the TE32 and TE33 complexes and a β-turn formed by the sequence IDSQ in the TE34 complex. The $^3J_{HN}$ coupling constants between the α and the amide protons of the same residue can be used to obtain restraints on the ϕ dihedral angles along the polypeptide backbone only when the chemical shifts of the bound and free ligand are averaged as a result of a fast exchange rate relative to the chemical shift differences. The $^3J_{HN}$ coupling constants for the bound peptide can be deduced from measurements using various ratios between free and bound peptide and extrapolating to zero concentration of the free peptide. This is not the case for the three antibody complexes that we have investigated.

Influence of Spin Diffusion. Experiments carried out using 30- and 60-ms mixing times ruled out the possibility that some of the cross-peaks that we observed with a 100-ms mixing time were due to spin diffusion. This larger mixing time was necessary to obtain a good signal-to-noise ratio for many cross-peaks. The absence of interference from spin diffusion in the experiments that we have carried out could be due to the following: (a) All the restraints were derived from experiments in which we used extensive deuteration of the aromatic amino acids of the antibody. In the experiments with TE34 all aromatic amino acids except histidine were deuterated, and in TE33 tryptophan and phenylalanine were perdeuterated and tyrosine was deuterated at C_δ positions. As the combining sites of all three antibodies are highly aromatic, many relaxation pathways that could lead to interresidue spin diffusion were blocked by antibody deuteration. (b) The rotational correlation time of the Fab was previously found to be 20 ns at room temperature (Anglister et al., 1984). All TRNOE experiments that were reported previously and that were used to derive restraints on intermolecular distances were carried out between 37 and 42 °C. The higher temperature probably reduces the rotational correlation time by as much as 40%, mainly due to the reduced viscosity of water, thus further decreasing the efficiency of spin diffusion. (c) In difference spectroscopy one observes only relatively strong cross-peaks, many of which represent distances shorter than 3 Å. In this range of distances and for the rotational correlation time at the elevated temperature and a mixing time of 100 ms, errors in evaluating interproton distances are minimal as shown by Campbell and Sykes (1991).

Size and Conformation of the Epitopes. There are several common features in the NMR-derived models for the three-dimensional structure of the three peptide–antibody complexes that we have determined and in the structure of another complex solved by crystallography (Stanfield et al., 1990). (a) The epitope consists of about eight residues. (b) The contact area between the two molecules is 350–500 Å^2, about 60% of that observed in protein–antibody complexes. (c) The peptide folds into a β-turn in all four anti-peptide antibodies. In TE32 and TE33 this turn is part of a larger loop. This compact folding maximizes the contact area between the peptide and the antibody and allows greater conformational freedom than α-helix or β-sheet secondary structure.

Mechanism of Antibody Interactions with Peptide Antigens. In the NMR spectra of free CTP3 we do not see any evidence for a preferred β-turn conformation in the sequence VPGS or IDSQ. The interactions between the amide protons of gly^5 and ser^6, and ser^{11} and gln^{12}, which are indicative of the β-turn in VPGS and IDSQ respectively, are weak and comparable to interactions between other pairs: ser^6 and gln^7,

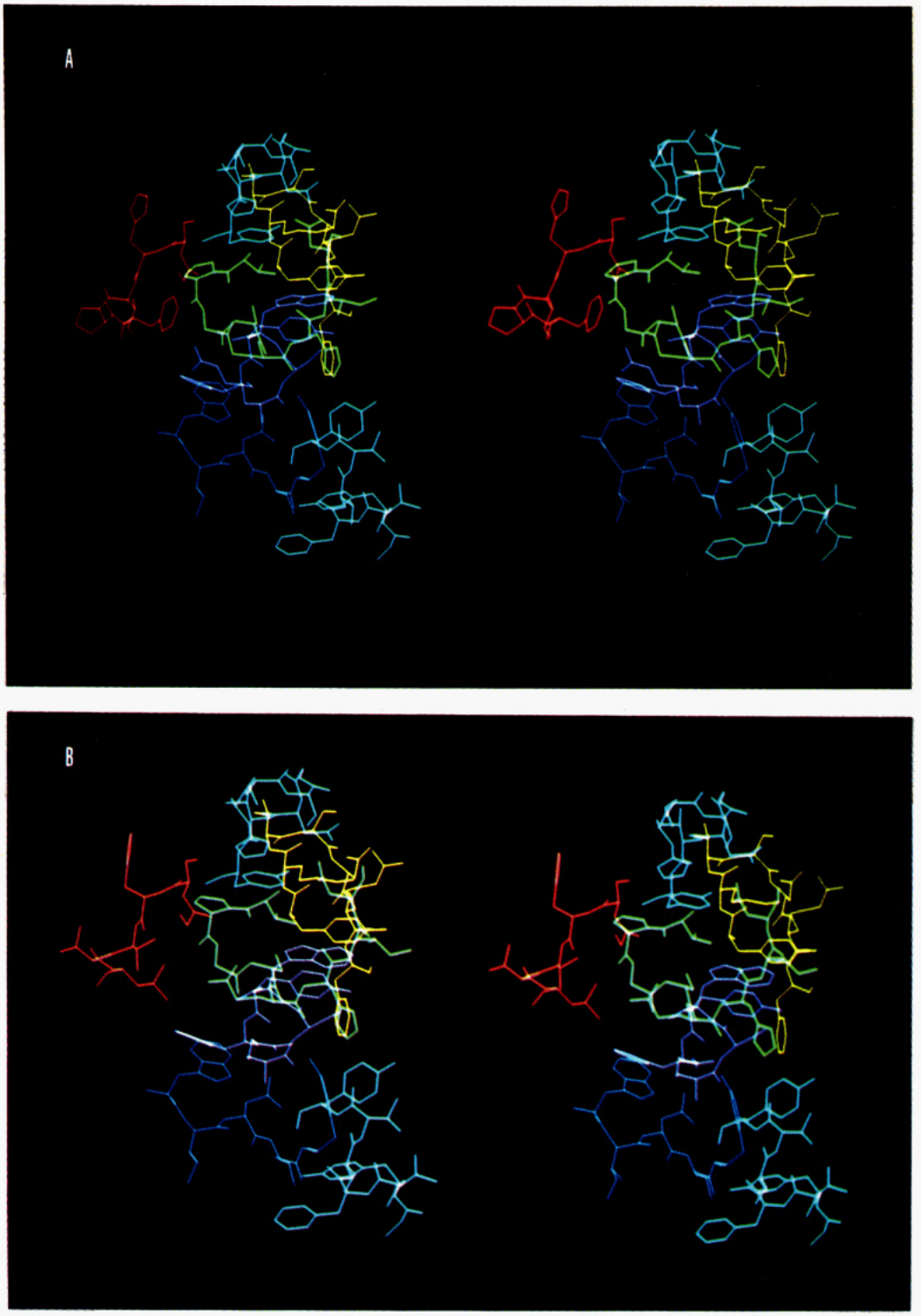

FIGURE 10: (A) Stereoview of the lowest energy structure of CTP3 bound to the combining site of TE33 obtained after energy minimization, restrained molecular dynamics, and simulated annealing calculations using NMR distance restraints and a preliminary model for the antibody Fv: light blue (top), yellow, and red, CDR 1, 2, and 3 of the light chain, respectively; light blue (bottom), blue, and purple, CDR 1, 2, and 3 of the heavy chain; light green, residues 3–10 of CTP3. (B) Corresponding structure of the TE32–CTP3 complex. The colors used represent the same regions as specified in (A).

gln^{7} and his^{8}, his^{8} and ile^{9}, asp^{10} and ser^{11}, and gln^{12} and lys^{13} (Figure 2). It is therefore concluded that when CTP3 is free in solution, it does not fold into a well-defined conformation, probably assuming a rapidly interconverting distribution of different conformations.

At room temperature the off-rate of CTP3 bound to TE33 is of the order of 1 s^{-1} (Anglister et al. 1988), and its binding constant is 1.2×10^{6} M^{-1}. Its on-rate, therefore, is approximately 10^{6} s^{-1}, which is slower than what is expected from a diffusion-controlled on-rate. The fact that the on-rate is about 2 orders of magnitude slower than a diffusion-controlled on-rate probably indicates peptide binding by an induced-fit mechanism in which the peptide folds into a conformation that is dictated by the much less flexible structure of the antibody (Dyson et al., 1988a). Immunization with peptides induces the proliferation of those B-cells carrying preexisting receptors into which the peptide can fold and create contacts that are energetically favorable. Our studies demonstrate that a short peptide can present different epitopes to the immune system and different bound peptide conformations

Table III: Contact Areas[a] between the Peptide and the TE33 Antibody

		contact area (in Å²) to									
loop	residue	val 3	pro 4	gly 5	ser 6	gln 7	his 8	ile 9	asp 10	total residues	total loop
						Light Chain					
CDR1	His 31	15	15						14	44	
	→Ser 31C[b]								15	15	
	Asn 31E								15	15	
	Tyr 32	14	5						8	27	101
CDR3	Ser 92		14							14	
	His 93		7							7	
	→Ile 94		20	7						27	
	→Phe 96			5		18				23	71
						Heavy Chain					
CDR1	→Thr 31						12			12	
	Tyr 32						22			22	34
CDR2	Trp 50			23	3	31				57	
	Tyr 53				17	14				31	88
CDR3	→Arg 95					7				7	
	→Ser 96					5	13			18	
	Trp 100A	13				21	40	13		87	112
total		42	61	35	20	96	87	13	52	406	406

[a] Contact areas are calculated using a variant of the method of Lee and Richards (1971) to calculate accessible surface area. In that method, the accessible surface area of an atom is that of a sphere of radius equal to the radius of the atom plus the radius of a water molecule (taken as 1.4 Å) minus the sum of contact areas with all adjacent atoms. These contact areas can overlap and are normalized by the actual total contact area after allowing for all overlap. Thus, the contact areas measured here sum to give the loss in accessible surface area of each atom or residue. The individual values indicate how much the contact of a particular pair of residues reduces the total solvent-accessible surface area. Contact areas smaller than 3 Å² are omitted for greater clarity. [b] Residues that are different in DB3 and TE33 are marked with an →.

Table IV: Contact Areas[a] between the Peptide and the TE32 Antibody

		contact area[c] (in Å²) to									
loop	residue	val 3	pro 4	gly 5	ser 6	gln 7	his 8	ile 9	asp 10	total residues	total loop
						Light Chain					
CDR1	His 31	12	19						9	40	
	→Ser 31C[b]								19	19	
	Asn 31E								6	6	
	Tyr 32	12							8	20	85
CDR3	Ser 92		14							14	
	Val 94		26			16				42	56
						Heavy Chain					
CDR1	→Thr 31						14			14	
	Tyr 32						18			18	32
CDR2	Trp 50			10		35				45	
	Tyr 53				7	8	4			19	64
CDR3	→Arg 95					22	12			34	
	→Ser 96						8			8	
	Trp 100A	15				13	34	3		65	107
total		39	59	10	7	94	90	3	42	344	344

[a] See footnote *a* to Table III. [b] See footnote *b* to Table III. [c] Energy values show the importance of the variable polar residue more clearly.

are induced upon binding to different antibodies.

Folding of a flexible peptide into a β-turn in the antibody complex was also demonstrated in studies of the conformation of a myohemerythrin peptide free in water and trifluoroethanol solutions (Dyson et al., 1988b) and bound to an antibody (Stanfield et al., 1990). Although multiple weak interactions between the amide protons of adjacent amino acids were observed in the sequence DFLEKIGGL (residues 11–19) of the peptide in aqueous solution and addition of TFE stabilized a helical conformation at the C-terminus, no interactions were observed in the N-terminal part (EVVPHKKMHK) of the 19-residue peptide in aqueous or TFE solution. The latter sequence includes the epitope that interacts with the antibody studied by Stanfield et al. (1990) and which assumes a β-turn in the bound state.

Implications for the Cross-Reactivity of Anti-Peptide Antibodies with Native Proteins. Arnon, Sela, and their coworkers have shown that anti-CTP3 serum partially neutralizes the biological activity of cholera toxin in vitro (Jacob et al., 1983, 1984). Anti-cholera toxin serum was found to have much stronger activity. In our experiments the monoclonal antibody TE33 failed to neutralize the biological activity of cholera toxin (Reuben Hiller, unpublished results), and its binding to cholera toxin in solution was 3 orders of magnitude weaker than its binding to the peptide. By following retardation in size-exclusion HPLC, Spangler (1991) could not detect TE33 and TE32 binding to cholera toxin in solution. However, this method cannot detect the very weak binding that we found in our ESR experiments. Previous studies from various groups found that the affinity of anti-peptide antibodies to the native protein is usually lower than the affinity to the immunizing peptide by 2–3 orders of magnitude (Berzofsky, 1985; Darseley at al., 1985; Hirayama et al., 1985). In view of the modest binding to the peptide and the very weak binding to cholera toxin, it is not surprising that TE33 does not neutralize cholera toxin. Unfortunately, TE33 was selected

on the basis of its strong cross-reactivity with cholera toxin in a solid-phase assay which apparently does not correlate well to its binding in solution. Therefore, the neutralization activity of anti-CTP3 serum must be attributed to antibodies that have much stronger binding to cholera toxin than do TE32 and TE33. The observed difference between the cross-reactivity of TE33 and TE32 and that of TE34 with cholera toxin in ELISA is mostly due to the fact that TE34 binding to CTP3 is 2 orders of magnitude weaker if the peptide's C-terminal carboxyl is modified into an amide. Since the TE34 epitope in intact cholera toxin ends with an amide bond to residue 65 of the B-subunit, it is not surprising that TE34 interacts very weakly with the protein. Given the above finding, a further search for the neutralizing activities in other anti-CTP3 monoclonal antibodies might prove very worthwhile.

Calculations made by Barlow et al. (1986) showed that, of the possible conformations for continuous protein epitopes, loops protruding from the surface have the highest probability of forming the large contact surfaces necessary for high antibody binding affinity. Therefore, synthetic peptides corresponding in sequence to such loops are potentially good immunogens for obtaining antibodies cross-reactive with native proteins. The three-dimensional structure of cholera toxin has not been published. However, Sixma et al. (1991) solved the structure of the heat-labile enterotoxin of *E. coli* (HLT) which shares 80% sequence homology with cholera toxin. CTP3 corresponds to residues 50–64 in both toxins, and anti-serum against CTP3 recognizes both cholera toxin and HLT. In HLT residues 51–58 (residues 2–9 of CTP3) form a flexible protruding loop. This loop connects a β-structure (residues 47–50) and a long α-helix (residues 59–78). The flexibility of this loop and its protrusion may explain the results of Jacob et al. (1983, 1984), who demonstrated that of several peptides covering the complete sequence of the B-subunit of cholera toxin CTP3 was the most potent in inducing anti-serum cross-reactive with cholera toxin.

It is interesting to compare the model for the TE33-bound CTP3 to the recently obtained structure for HLT. Superposition of CTP3 bound to TE33 and the corresponding sequence of HLT shows the following: (a) The side chains of gln^7, his^8, and asp^{10} in HLT point toward the solvent and could interact with an antibody. (b) There is a good fit between our model and the HLT structure with respect to the conformation of the side chain of gln^7 and its orientation relative to the peptide backbone. (c) The orientation of the side chain of ile^9 is very similar in our model and in HLT. (d) Overall, the segment GSQHID has similar conformations in our model and in HLT, but for good superposition, the his^8 imidazole requires about a 90° rotation. (e) There are differences in the conformation of the sequence VP, and the β-turn VPGS is not observed in HLT. The rms deviation between the conformation of the antibody-bound epitope and the corresponding part of HLT is 2.6 Å. The actual binding of the antibody to the epitope on HLT may require a slight tilt of the loop to further expose the histidine imidazole to enable its interaction with the hydrophobic pocket in the antibody combining site. Bearing in mind that the epitope recognized by TE33 and TE32 corresponds to a flexible protruding loop in HLT and that the conformation of the sequence GSQHID is similar in the antibody-bound peptide and in HLT, one can expect that the flexible loop in HLT and in cholera toxin, if indeed its three-dimensional structure proves to be similar to that of HLT, can fold itself to the conformation recognized by TE33. As the conformations are not identical, such folding is probably accompanied by a positive contribution to the free energy of binding resulting in the observed decrease in the binding constant of TE33 to cholera toxin. If in solution the peptide adopts a stable conformation similar to that of the corresponding part of the protein, a higher degree of cross-reactivity with the native protein is expected. Such antibodies elicited against neutralizing epitope may have stronger neutralizing activity.

Relationship between Antibody Primary Structure and Function of the Antibody Combining Site. A computer search in antibody sequences reveals that Tyr 32L is invariant in all light chain sequences that share more than 65% sequence identity with TE33 (94 antibodies were found in this search). Tyr 32H and Trp 50H are invariant in all heavy chains, sharing more than 75% sequence identity with TE33 (25 antibodies). We have previously pointed out that Tyr 32L, Tyr 32H, and Trp 50H interact with the peptide antigen in all three anti-peptide antibodies that we have studied although TE34 recognizes a peptide segment that is different from that recognized by TE32 and TE33 (Zilber et al., 1990). Tyr 32L and Tyr 32H interact with the antigen also in the D1.3 complex with lysozyme (Amit et al., 1986). This conservation indicates that a mutation in these three aromatic residues in the highly homologous antibodies probably destroys the capability of the antibodies to bind antigens and/or may have severe implication on their folding to functional antibodies. The central location of the side chains of these residues in the antibody combining site and the fact that they interact with different antigens in different antibodies indicate that their role is to participate in nonspecific hydrophobic interactions with the antigen.

In all three anti-CTP3 antibodies that we have studied, CDR1 of the light chain has the same canonical conformation (Chothia & Lesk, 1987; Chothia et al., 1989). The side chains of residues 31, 31c, 31e, and 32 interact with the antigen in all three complexes. His 31L, Ser 31c, and Asn 31e in TE32 and TE33 are replaced by Asp 31L, Asp 31c, and Lys 31e, respectively, which are involved in electrostatic interactions in the TE34 complex. These findings imply that the folding of the CDR and its length dictate the positions in the sequence that interact with the antigen. In CDRs that have the same length and conformation, the side chains in these fixed positions have the potential to interact with the antigen.

The difference in the specificity between TE34 and the two other anti-CTP3 antibodies seems to arise from two main reasons: (a) Several mutations involving mostly polar interactions, for example, the mutations in CDR1 of the light chain, enable the specific recognition of the C-terminal carboxyl and the positively charged ϵ-amine of lys^{13}. (b) Changes in the length of CDR3 of the heavy chain cause major changes in the shape of the combining site accompanied by changes in hydrophobic and polar interactions with the antigen. Amino acid sequence comparison with the highly homologous heavy chain reveals that CDR3 of the heavy chain varies considerably in its length and amino acid sequence. The deletion of three CDR3 residues including Trp 100aH changed the shape of the combining site from a circular groove into a deep cavity.

ACKNOWLEDGMENT

We are greatly indebted to Prof. Ruth Arnon and Dr. Chaim Jacob for the gift of the TE32, TE33, and TE34 hybridomas, to Dr. Ian Wilson for allowing us to use the coordinates of DB3 before their general release, and to Drs. Hol and Sixma for sending us the coordinates of HLT. We are thankful for the use of the amino acid sequence data in the following banks:

Swiss protein, Genepept (Genebank), and Protein Identification Resource.

REFERENCES

Amit, A. G., Mariuzza, R. A., Phillips, S. E. V., & Poljak, R. J. (1986) *Science 233*, 747–753.

Anglister, J., & Zilber, B. (1990) *Biochemistry 29*, 921–928.

Anglister, J., Frey, T., & McConnell, H. M. (1984) *Biochemistry 23*, 1138–1142.

Anglister, J., Bond, M. W., Frey, T., Leahy, D., Levitt, M., McConnell, H. M., Rule, G. S., Tomasello, J., & Whittaker, M. (1987) *Biochemistry 26*, 6058.

Anglister, J., Jacob, C. O., Assulin, O., Ast, G., Pinker, R., & Arnon, R. (1988) *Biochemistry 27*, 717.

Anglister, J., Levy, R., & Scherf, T. (1989) *Biochemistry 28*, 3360.

Arnon, R. (1986) *Trends Biochem. Sci. 11*, 521–524.

Barlow, D. J., Edwards, M. S., & Thornton, J. M. (1986) *Nature 322*, 747.

Berzofsky, J. (1985) *Science 229*, 932.

Campbell, P. A., & Sykes, B. D. (1991) *J. Magn. Reson. 93*, 77–92.

Chothia, C., & Lesk, A. M. (1987) *J. Mol. Biol. 196*, 901–917.

Chothia, C., Lesk, A. M., Tramontano, A., Levitt, M., Smith-Gill, G. A., Sheriff, S., Padlan, E. A., Davies, D., Tulip, W. R., Colman, P. M., Spinelli, S., Alzari, P. M., & Poljak, R. J. (1989) *Nature 342*, 877.

Clore, G. M., Gronenborn, A. M., Carlson, G., & Meyer, E. F. (1986) *J. Mol. Biol. 190*, 259–267.

Colman, P. M., Laver, W. G., Varghese, J. N., Baker, A. T., Tulloch, P. A., Air, G. M., & Webster, R. G. (1987) *Nature 326*, 358–363.

Darsley, M. J., & Rees, A. R. (1985) *EMBO J. 4*, 383.

Deverson, E., Berek, C., Taussig, M., & Feinstein, A. (1987) *Eur. J. Immunol. 17*, 9–13.

Dwek, R. A., Wain-Hobson, S., Dower, S., Gettins, P., Sutton, B., Perkins, S. J., & Givol, D. (1977) *Nature 266*, 31–37.

Dyson, H. J., Lerner, R. A., & Wright, P. E. (1988a) *Annu. Rev. Biophys. Biophys. Chem. 17*, 305.

Dyson, H. J., Rance, M., Houghten, R. A., Wright, P. E., & Lerner, R. A. (1988b) *J. Mol. Biol. 201*, 20.

Epp, O., Lattman, E. E., Schiffer, M., Huber, R., & Palm, W. (1975) *Biochemistry 14*, 4943.

Furey, W., Jr., Wang, B. C., Yoo, C. S., & Sax, M. (1983) *J. Mol. Biol. 167*, 661.

Gaffney, B. J. (1976) *Spin Labeling Theory and Applications* (Berliner, L. J., Ed.) pp 184–238, Academic Press, New York.

Hirayama, A., Takagaki, Y., & Karush, F. (1985) *J. Immunol. 134*, 3241.

Jacob, C. O., Sela, M., & Arnon, R. (1983) *Proc. Natl. Acad. Sci. U.S.A. 80*, 7611.

Jacob, C. O., Sela, M., Pines, M., Hurwitz, S., & Arnon, R. (1984) *Proc. Natl. Acad. Sci. U.S.A. 81*, 7893.

Jones, T. A. (1978) *J. Appl. Crystallogr. 11*, 268.

Lee, B., & Richards, F. H. (1971) *J. Mol. Biol. 55*, 379.

Levitt, M. (1983a) *J. Mol. Biol. 168*, 595–620.

Levitt, M. (1983b) *J. Mol. Biol. 168*, 621–657.

Levy, R., Assulin, O., Scherf, T., Levitt, M., & Anglister, J. (1989) *Biochemistry 28*, 7168.

Macura, S., & Ernst, R. R. (1980) *Mol. Phys. 41*, 95–117.

Marquart, M., Deisenhofer, J., Huber, R., & Palm, W. (1980) *J. Mol. Biol. 141*, 369.

Padlan, E. A., Silverton, E. W., Sheriff, S., Cohen, G. H., Smith-Gill, S. J., & Davies, D. R. (1989) *Proc. Natl. Acad. Sci. U.S.A. 86*, 5938–5942.

Piantini, U., Sørensen, O. W., & Ernst, R. R. (1982) *J. Am. Chem. Soc. 104*, 6800–6801.

Plateau, P., & Gueron, M. (1982) *J. Am. Chem. Soc. 104*, 7310–7311.

Satow, Y., Cohen, G. H., Padlan, E. A., & Davies, D. R. (1987) *J. Mol. Biol. 190*, 593.

Saul, F. A., Amzel, L. M., & Poljak, R. J. (1978) *J. Biol. Chem. 253*, 585–595.

Sheriff, S., Silverston, E. W., Padlan, E. A., Cohen, G. H., Smith-Gill, S. J., Finzel, B. C., & Davies, D. R. (1987) *Proc. Natl. Acad. Sci. U.S.A. 84*, 8075.

Sixma, T. K., Pronk, S. E., Kalk, K. H., Wartna, E. S., van Zanten, B. A. M., Witholt, B., & Hol, W. G. J. (1991) *Nature 351*, 371–377.

Spangler, B. D. (1991) *J. Immunol. 146*, 1591–1595.

Stanfield, R. L., Fieser, T. M., Lerner, R. A., & Wilson, I. A. (1990) *Science 248*, 712–719.

Steward, M. W., & Howard, C. R. (1987) *Immunol. Today 8*, 51–58.

Stura, E. A., Feinstein, A., & Wilson, I. A. (1987) *J. Mol. Biol. 193*, 229–231.

Suh, S. W., Bhat, T. N., Navia, M. A., Cohen, G. H., Rao, D. N., Rudikoff, S., & Davies, D. R. (1986) *Proteins: Struct., Funct., Genet. 1*, 74.

Theriault, T. P., Leahy, D. J., Levitt, M., & McConnell, H. M. (1991) *J. Mol. Biol. 221*, 257–270.

Wüthrich, K., Billeter, M., & Braun, W. (1983) *J. Mol. Biol. 169*, 949–961.

Zilber, B., Scherf, T., Levitt, M., & Anglister, J. (1990) *Biochemistry 29*, 10032.